

Total β -decay energies and masses of strongly neutron-rich indium isotopes ranging from ^{120}In to ^{129}In

K. Aleklett, E. Lund, and G. Rudstam

The Studsvik Science Research Laboratory, Studsvik, Fack, S-611 01 Nyköping, Sweden

(Received 19 December 1977)

Experimental total β -decay energies of strongly neutron-rich indium isotopes are presented. The samples were produced as mass-separated fission products by using the on-line isotope separator technique. By means of a Si(Li)-detector system, β spectra were recorded in coincidence with different γ gates, and Q_β values for isomers of $^{120-129}\text{In}$ were deduced. The atomic mass excess is derived for these nuclei, and comparisons are made with mass formula predictions. The mean uncertainty of the experimental mass excesses is 0.11 MeV. The precision of the mass formulas chosen for the comparison varies widely with rms deviations ranging from 0.21 to 1.36 MeV. For the isotopes $^{124-129}\text{In}$ the possibility of delayed-neutron emission is discussed.

RADIOACTIVITY $^{120-129}\text{In}$: Measured β - γ coincidences for isomers; deduced total β -decay energies, atomic mass excesses, delayed-neutron windows; comparison with mass formulas. Mass-separated fission products, Si(Li)-detectors, Ge(Li)-detector, NaI(Tl)-detectors.

I. INTRODUCTION

A fundamental property of the atomic nucleus is its mass. The ISOL technique¹ has made an increasing number of nuclides far from the region of β stability available for mass determinations. The most accurate measurements of stable nuclides have been performed with mass spectrometers, and recently such determinations of radioactive neutron-deficient rubidium isotopes were reported² with the spectrometer connected to ISOLDE at CERN. The uncertainties of the latter measurements are reported to be 25–80 keV. So far, direct mass determinations are limited to a few elements by the restriction that no other isobars or isomers are allowed to be present in the samples. This means that accurate direct mass determinations will be extremely difficult to perform for the neutron-rich indium isotopes of interest in this work because of the presence of isomerism. The indirect method of determining the mass differences from nuclear decay energies (Q_β values), adopted in the present study, is therefore the only realistic alternative.

Beside the general importance of masses and Q_β values, mass data of neutron-rich nuclides are of special interest as these data are essential for the construction of mass formulas used in the theories of nucleosynthesis³ and for predictions about superheavy elements.

The isotope-separator facility OSIRIS⁴ connected to the R2-0 reactor at Studsvik is an excellent tool for producing neutron-rich fission products. With this equipment it has been possible to

study indium isotopes ranging from ^{117}In to ^{132}In . In this article Q_β values and mass excesses covering the mass range 120–129 are presented. The technique used in these experiments is described in Sec. II, and in Sec. III the results of the Q_β measurements are reported. Finally, the experimental Q_β values and corresponding mass excesses are compared with predictions from different mass formulas in Sec. IV. In the same section the application of experimentally measured Q_β values to the identification of delayed-neutron precursors is described.

II. EXPERIMENTAL TECHNIQUES

A. On-line mass separation and sample production

At the OSIRIS facility, indium isotopes are produced by thermal-neutron induced fission of ^{235}U . A cylinder consisting of several layers of graphite cloth is impregnated with about 3 g of the target material and enclosed in the ion source of the isotope separator.⁵ The recoiling fission fragments are caught in the graphite, diffuse to the surface, evaporate, and finally, get ionized and separated in a 55° fringing-field type of magnet.⁶ There is very slight element selection in the system, and the samples contain generally two or more isobars which have to be separated by a proper timing of the experiment and also by choosing selective coincidence conditions.

The activities were collected on tape, either in the collector chamber of the separator or at a tape position at the end of a beam line. The collector chamber tape system needed a trans-

portation time of 3 s,⁷ while the other tape system transports the sample to the detector system within 0.3 s.

In the present work the uranium target was irradiated in a neutron flux of about $10^{10} n_{\text{th}}\text{cm}^{-2} \text{ s}^{-1}$ (the available neutron flux is $4 \times 10^{11} n_{\text{th}}\text{cm}^{-2} \text{ s}^{-1}$).

B. Detector arrangements

The basic principle for the determination of total β decay energies is to measure β branches to known excited states of the daughter nucleus. For this purpose a $\beta\gamma$ -coincidence spectrometer (Q_β spectrometer) has been constructed. It consists of a system of Si(Li) detectors for β detection and two NaI(Tl) detectors, or a Ge(Li) detector, for γ detection.

Three different detector configurations have been used in the present experiment.

Method I: a main Si(Li) detector surrounded by three anticoincidence Si(Li) detectors for β measurement and two NaI(Tl) detectors for γ measurement; transport time 3 s.

Method II: a main Si(Li) detector surrounded by two anticoincidence Si(Li) detectors for β measurement and two NaI(Tl) detectors for γ measurement; transport time 0.3 s.

Method III: a main Si(Li) detector surrounded by two anticoincidence Si(Li) detectors for β measurement and a Ge(Li) detector for γ measurement; transport time 0.3 s.

In all experiments the same main Si(Li) detector was used: a 25 mm diam \times 5 mm thick transmission detector from which a segment has been cut from the detector itself in such a way that the β particles from a sample will see a sensitive depth up to 23 mm. This corresponds to the range of electrons of energy about 10 MeV. Method I is described in detail in Ref. 7 and will not be further discussed here. In Fig. 1 a block diagram of method II is shown, and the Ge(Li) detector used in method III is also indicated. The response function and the efficiency of the Si(Li) system are discussed in Sec. II E. Method III is described in Ref. 8.

C. Experimental procedures

As no chemical separation was used, the mass-separated samples contained in addition to indium, isobaric components consisting of isotopes of cadmium and/or tin. The situation is favorable for the indium isotopes, however, which could in most cases be enhanced by a proper timing of the experiment. For those indium isotopes measured by method III no problem with contamination arises as the γ gates are chosen in a well resolved spectrum measured by a Ge(Li) detector.

Experimentally, it has been found that a counting rate of up to 4000 cps in the main β detector gives a β spectrum free from pileup. This sample strength also gives a suitable counting rate in the γ detectors. The reactor power was adjusted to give this sample intensity. Usually, $(5-10) \times 10^7$ β events were collected in the main detector in order to make possible an accurate Fermi-Kurie (FK) analysis of the coincident β spectra.

The treatment of the 0.9 s activity of ^{129}In will now be discussed as an example of method II. The daughter ^{129}Sn has such a long half-life, 134 s, compared to ^{129}In , that negligible influence is expected with a collection time of 2 s. About 15 000 samples were collected and measured during the experiment. The γ spectrum obtained for a few hundred samples is shown in Fig. 2. A γ line corresponding to a ground state transition of 2119

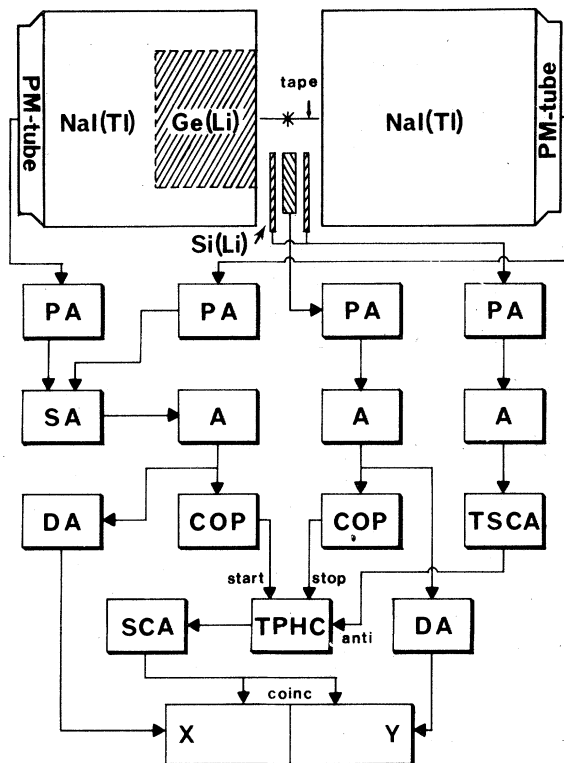


FIG. 1. Block diagram of the electronics used for counting β - γ coincidences with method II. The Ge(Li) detector used in method III is also indicated. (PA = preamplifier; SA = sum amplifier; A = amplifier; DA = delay amplifier; COP = crossover pickoff; TSCA = timing single channel analyzer; SCA = single channel analyzer; TPHC = time-to-pulse-height converter; X and Y = analog-to-digital converters.) A star indicates the position of the sample.

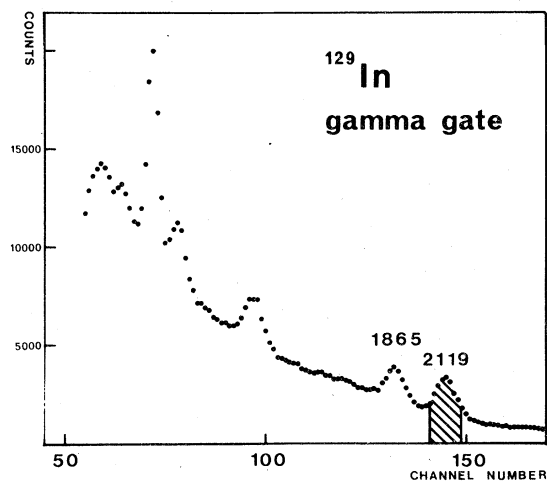


FIG. 2. The γ spectrum of the mass chain 129 recorded with NaI(Tl) detectors. The γ gate chosen for the coincident β spectrum is shaded.

keV was chosen as a gate for the β spectrum (see Fig. 4) and the coincident β events were stored directly in the analyzer memory. The time resolution was about 80 ns. The accidental coincidence spectrum obtained by displacing the time window in the coincidence circuit was subtracted, and the true β -pulse spectrum was then transformed to an electron distribution (see Sec. II E). In this case the background effect was negligible.

In method III the narrow time window, 19 ns, makes the accidental coincidence rate negligible at the counting rates used. In this case also the pulses in an energy interval close to each γ gate of width corresponding to that of the gate itself were recorded. The spectra thus obtained were subsequently subtracted from the β spectra coincident with the γ gates to give a background correction.

D. Calibration of the β detector

The linearity of the β detector has been investigated using conversion electrons from ^{207}Bi and from the daughters of ^{228}Th .⁷ These cover the energy interval from 0.5 to 2.6 MeV. Within this interval the main Si(Li) detector was linear. The electronic system was controlled with a pulse generator and found to be linear at least up to 10 MeV. The maximum deviation from a line defined by the ^{207}Bi conversion electron peaks was 4 keV in the range 1.68–10 MeV.

During the experiments only ^{207}Bi was used as a calibration source, and a linear fit to the three conversion electron lines was used as a calibration line in the analysis.

The adopted Q_β values, 3.889 ± 0.005 of ^{87}Kr and

3.541 ± 0.009 MeV of ^{106}Rh ,⁹ were used as check points of the calibration. Our results were for ^{87}Kr $Q_\beta = 3.87 \pm 0.09$ MeV and for ^{106}Rh $Q_\beta = 3.55 \pm 0.07$ MeV.⁸

E. Data analysis

The pulse distributions coincident with different γ gates were analyzed by means of a computer program in order to determine the end points of the energy spectra from a Fermi-Kurie plot. In a first step the pulse distribution was transformed to an electron distribution, and in a second step the FK parameter $(N/pWF)^{1/2}$ was calculated where N is the transformed electron intensity, p and W are the relativistic electron momentum and energy, respectively, and F is the Fermi function. A weighted least squares fit to these points gave the E_β^{max} and, by adding the level energy, the total β -decay energy was deduced.

For the transformation one needs to know the response and the efficiency functions for the β detector. The response function was determined using the ^{207}Bi conversion electron spectrum, and a good approximation was found to be a Gaussian full energy peak (full width at half maximum = 12 keV) with a constant tail down to zero energy.⁸ Within the energy range covered, 0.48–1.68 MeV, the peak-to-total ratio was found to be 0.30 and independent of electron energy.⁸ Berger *et al.*¹⁰ have made an extensive study of the response function for various types of Si(Li) detectors. They concluded that the peak-to-total ratio was almost constant for energies from 1 to 5 MeV. They also found that the tail down to zero energy was constant even for 5 MeV electrons. In the transformation from pulse distribution to electron distribution a channel width of at least 35–40 keV was chosen. The Gaussian peak then appears in a single channel, which makes the error analysis of the transformation very simple.⁸

The efficiency function of the β -detector system depends mainly on the anticoincidence condition, but also to a certain extent on the response function used. In the energy range 0.48 to 1.68 MeV the conversion electron spectrum of ^{207}Bi can be used for an efficiency check. The ratio of the peak intensities for the lines 1681 and 481 keV recorded with our system was 0.012 ± 0.001 , in agreement with 0.012 ± 0.001 from Ref. 11. Thus, in this energy range the efficiency was constant.

The odd-mass indium isotopes provide an excellent possibility to determine the efficiency above 1.68 MeV. One can find several coincident β spectra consisting of only one component. The end points of these branches are between 3.2 and 5.4 MeV. The experimental β spectra were trans-

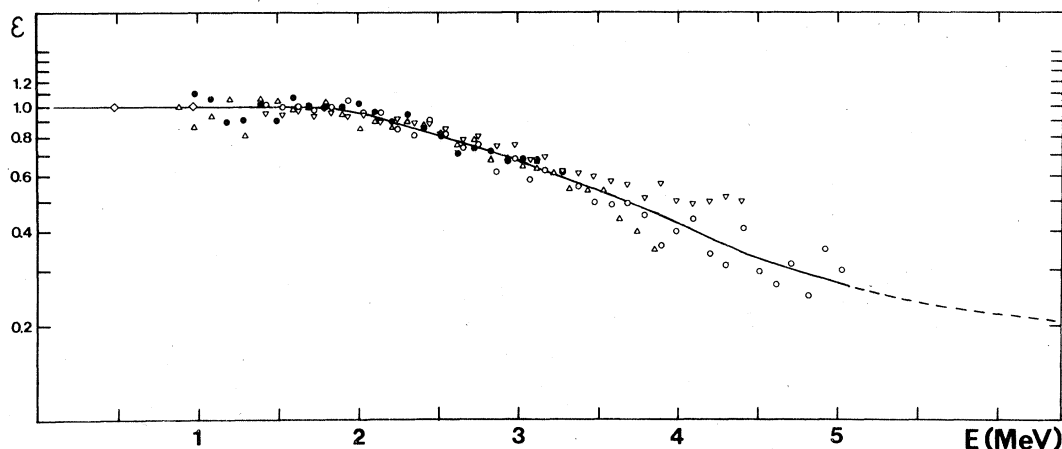


FIG. 3. The efficiency function of the Si(Li) system. The experimentally determined points are represented by \diamond (^{207}Bi), \bullet (^{123}In), \triangle (^{125}In), ∇ (^{127}In), and \circ (^{129}In). The uncertainties of the experimental points around 1.5 MeV are between 0.05 and 0.07, while an uncertainty between 0.10 and 0.15 is valid for the high energy parts. The solid line represents a fifth degree polynomial fitted to the experimental points.

formed with the response function described above and a constant efficiency yielding a first order approximation of E_{β}^{max} . Using this value a theoretical β spectrum was calculated, and the ratio between the transformed and the calculated electron distributions gives a new set of efficiency values to be used for a second-order approximation of E_{β}^{max} . The procedure was then repeated until no further changes occurred. The resulting efficiency function is shown in Fig. 3. For more details see Ref. 8.

When more than one determination of the Q_{β} value of a nuclide were made, the mean value was calculated with its uncertainty given as

$$\sigma = [\bar{\sigma}^2 + \sigma^2(E_{\text{cal}})]^{1/2}, \quad (1)$$

where

$$\bar{\sigma} = \left(\sum_i \sigma_i^{-2} \right)^{-1/2}, \quad (2)$$

and $\sigma(E_{\text{cal}})$ equals the largest calibration uncertainty for the determinations.

The expression (2) was chosen because in all cases it gave values larger than the error deduced from the external consistency of the points. The nonlinearity of the system⁸ was found to introduce negligible error (maximum error 4 keV).

III. EXPERIMENTAL RESULTS

The level structure of tin isotopes has been studied in the mass interval 119–132,^{12–17} and the half-lives of the isotopes of indium have been determined by means of β , γ , and delayed-neutron counting.^{18,19}

A. Odd-mass indium isotopes

1. Nuclides ^{121}In , ^{123}In , and ^{125}In

The decay properties of odd-mass indium isotopes in the mass range 119–125 have been thoroughly investigated by Fogelberg *et al.*¹² A characteristic feature of these nuclides is the presence of two isomers about 300 keV apart.¹³ The spin and parity assignment is $\frac{9}{2}^+$ for the ground states and $\frac{1}{2}^-$ for the isomeric states. Partial level schemes of odd-mass tin isotopes from Refs. 12, 14 are shown in Fig. 4. For determinations of total β decay energies of the ground states, the γ transitions 926 keV in ^{121}Sn , 1020 and 1131 keV in ^{123}Sn , and 1032 and 1335 keV in ^{125}Sn were chosen as gates for the β spectra. These γ transitions depopulate the $\frac{7}{2}^+$ states which are strongly favored (95–100%) in the β decay. Therefore the coincident β spectra consist of only one component, which makes a linear fit possible over a wide energy range in the FK analysis.

The isomeric states mainly decay to low-lying states in the daughter nuclei. In ^{121}Sn the $\frac{1}{2}^+$ state is situated at 60 keV which is below our limit for γ gates. The transitions between the $\frac{1}{2}^+$ and the $\frac{3}{2}^+$ states in ^{123}Sn and ^{125}Sn of energy 126 and 188 keV, respectively, were chosen as γ gates for the first forbidden β spectra from the isomeric states in ^{123}In and ^{125}In . Lacking proper shape factors the spectra were treated as allowed ones in the analysis.

Method I (cf. Sec. II B) was used for ^{121}In and method III for ^{123}In and ^{125}In .

The experimental results are collected in Table I. The Q_{β} value has been deduced for each β

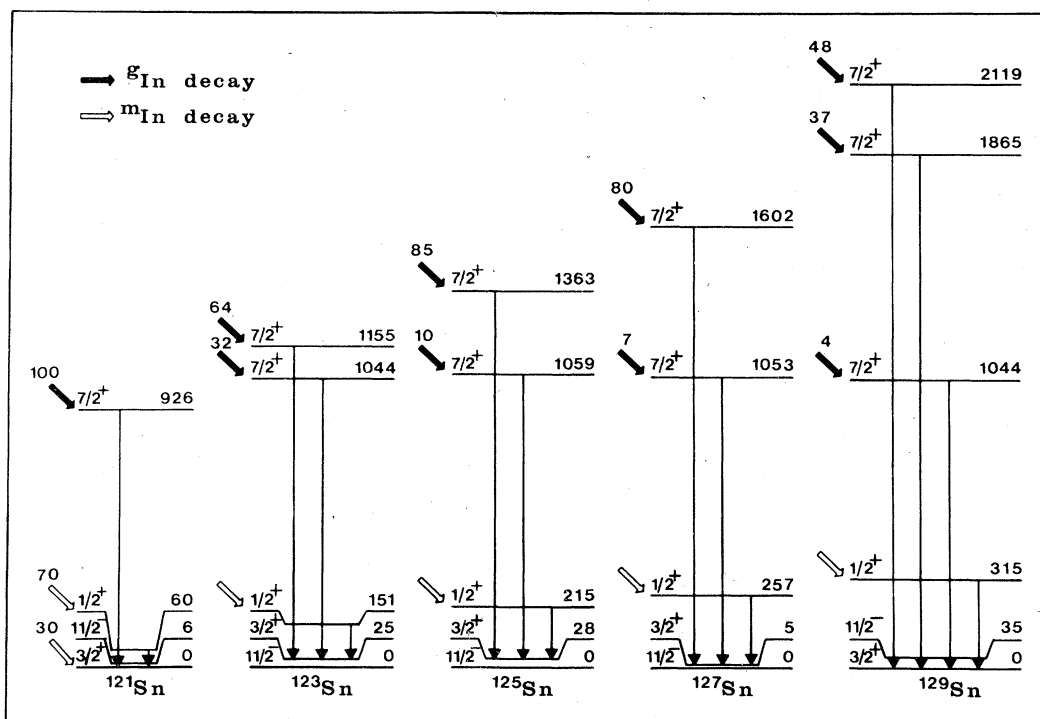


FIG. 4. Partial level schemes for odd-mass tin isotopes.

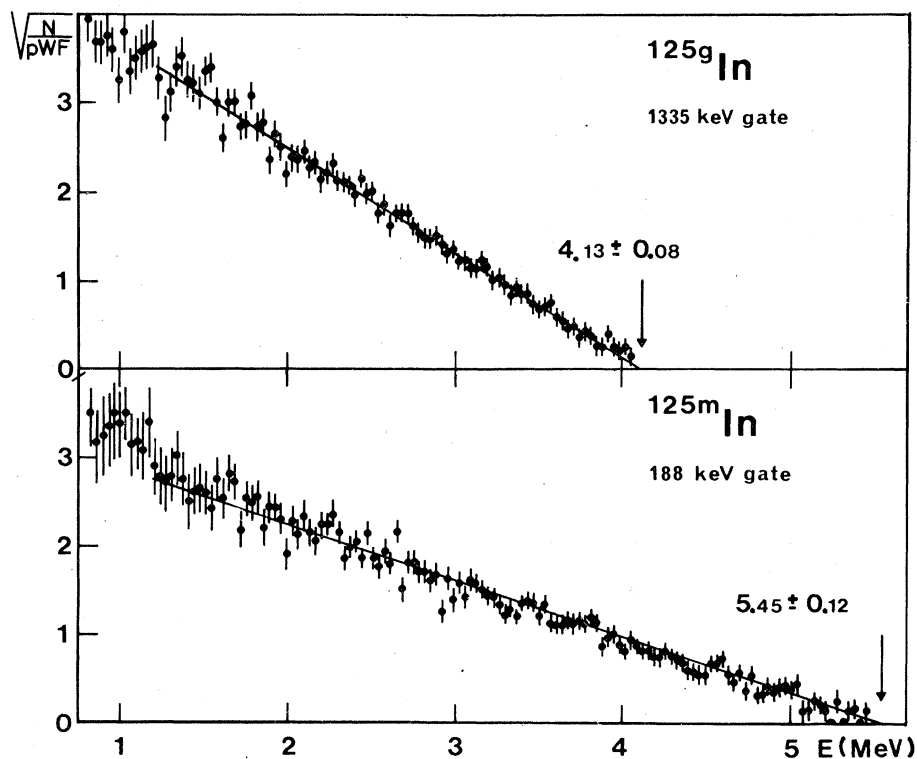


FIG. 5. Fermi-Kurie plots of the β spectra corresponding to the 1335 and 188 keV gates which depopulate the levels at 1363 and 215 keV in ^{125}Sn . These levels are fed by β particles from the ground state and the isomeric state of ^{125}In , respectively.

TABLE I. Results of FK analyses for the odd-mass indium isotopes ^{121}In , ^{123}In , ^{127}In , and ^{129}In

Nuclide	Method	Half-life (s)	Gate energy (keV)	Level (keV)	Range of fit (MeV)	E^{\max} (MeV)	Q_{β} value (MeV)	Mean Q_{β} value (MeV)	Other experimental determinations (MeV)
$^{121}\text{In}^g$	I	23.1 ^a	926	926 ^b	1.2-2.4	2.48 \pm 0.05	3.41 \pm 0.05		3.38 \pm 0.04 ^c
$^{121}\text{In}^m$		233 ^a					3.72 \pm 0.05 ^d		
$^{123}\text{In}^g$	III	5.98 ^a	1020 1131	1044 ^b 1155	1.2-3.2 1.0-3.2	3.36 \pm 0.10 3.30 \pm 0.07	4.40 \pm 0.10 4.46 \pm 0.07	4.44 \pm 0.06	4.38 \pm 0.05 ^e
$^{123}\text{In}^m$	III	47.8 ^a	126	150 ^b	1.0-4.4	4.54 \pm 0.21	4.69 \pm 0.21		
$^{125}\text{In}^g$	III	2.33 ^a	1032 1335	1059 ^b 1363	1.5-4.2 1.5-4.0	4.34 \pm 0.28 4.13 \pm 0.08	5.40 \pm 0.28 5.49 \pm 0.08	5.48 \pm 0.08	
$^{125}\text{In}^m$	III	12.2 ^a	188	214 ^b	1.2-5.2	5.45 \pm 0.12	5.66 \pm 0.12		
$^{127}\text{In}^g$	II	1.3 ^a	1597 1597	1602 ^f 1602	1.2-4.8 1.2-4.8	4.86 \pm 0.08 4.99 \pm 0.16	6.46 \pm 0.08 6.59 \pm 0.16	6.49 \pm 0.07	
$^{127}\text{In}^m$	II	3.7 ^a	252 252	257 ^f 257 ^f	4.5-6.1 4.5-6.1	6.37 \pm 0.28 6.41 \pm 0.24	6.63 \pm 0.28 6.67 \pm 0.24	6.65 \pm 0.18	
$^{129}\text{In}^g$	II	0.9 ^f	2119	2119 ^f	1.5-5.3	5.48 \pm 0.12	7.60 \pm 0.12		
$^{129}\text{In}^m$	II	1.2 ^f	315	315 ^f	5.0-7.5	7.5 \pm 0.6	7.8 \pm 0.6		

^aReference 18.^bReference 12.^cReference 9.^dObtained by adding the isomeric transition energy to the Q_{β} value for $^{121}\text{In}^g$.^eReference 20.^fReference 14.

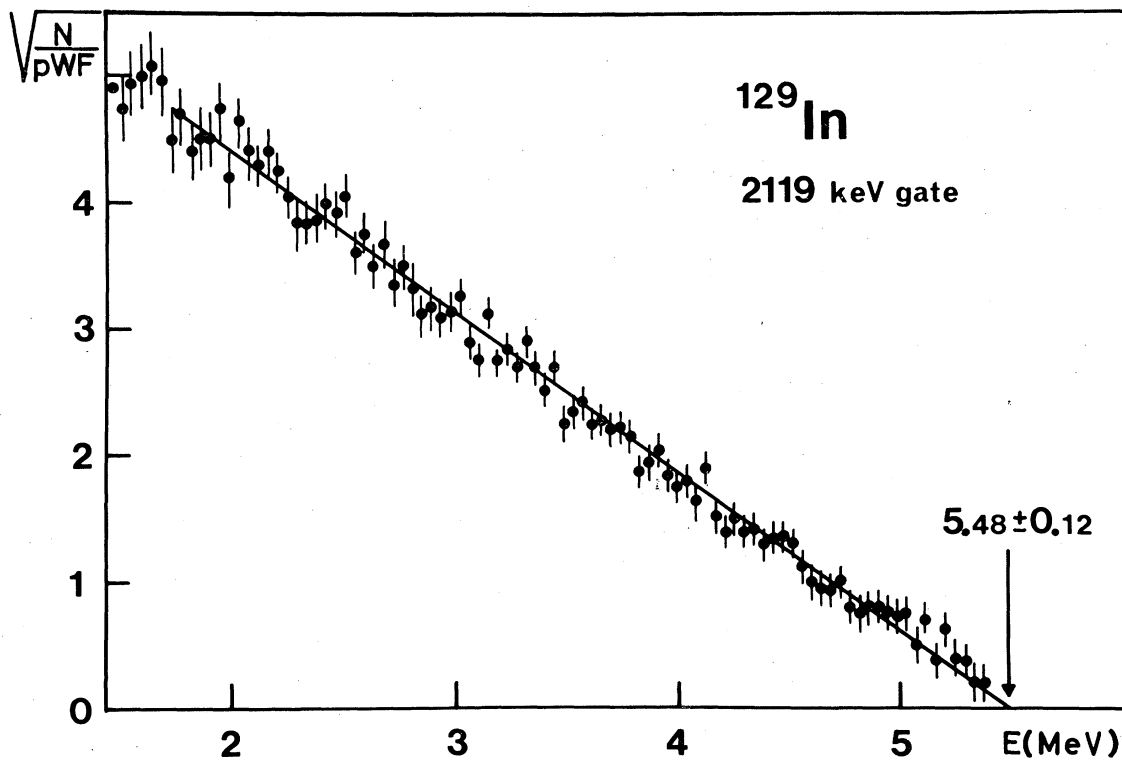
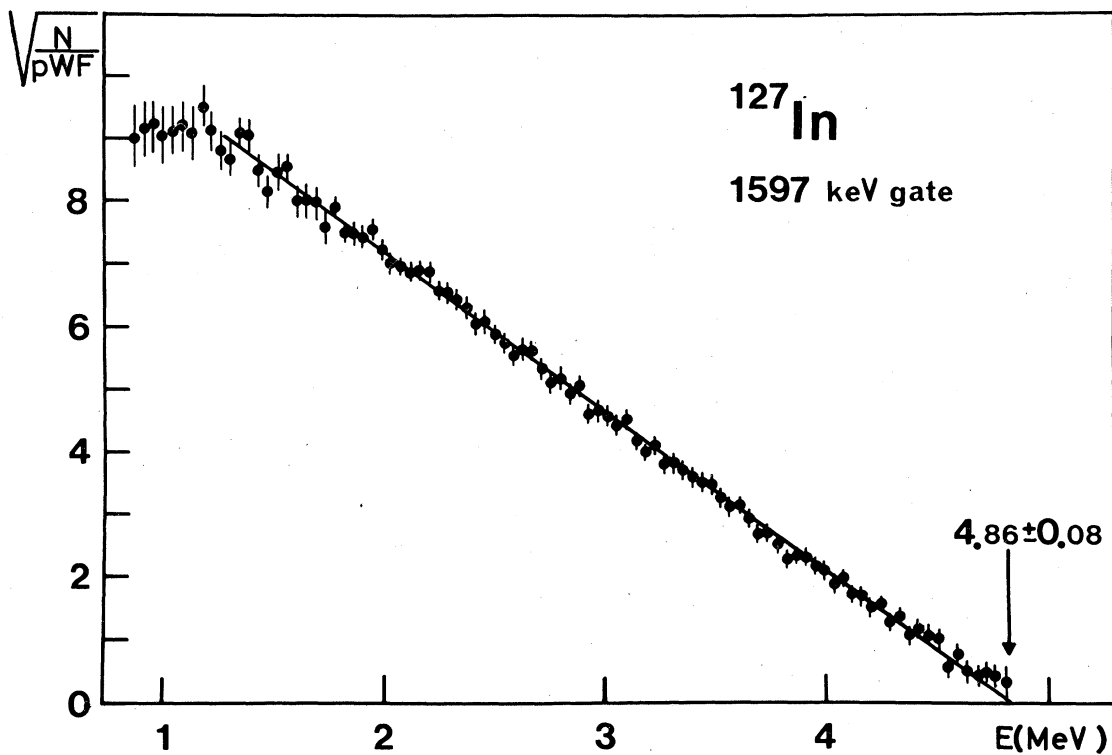


FIG. 6. Fermi-Kurie plots of the β spectra corresponding to the 1597 keV (a) and 2119 keV (b) gates. These γ transitions depopulate the levels at 1602 and 2119 keV in ^{127}Sn and ^{129}Sn , respectively.

branch, and for cases where more than one determination is made the average value has been calculated. The main results are $^{121}\text{In}^g$, $Q_\beta = 3.41 \pm 0.05$ MeV, $^{123}\text{In}^g$, $Q_\beta = 4.44 \pm 0.06$ MeV, $^{123}\text{In}^m$, $Q_\beta = 4.69 \pm 0.21$ MeV, $^{125}\text{In}^g$, $Q_\beta = 5.48 \pm 0.08$ MeV, and $^{125}\text{In}^m$, $Q_\beta = 5.66 \pm 0.12$ MeV.

The Q_β values for $^{121}\text{In}^g$ and $^{123}\text{In}^g$ are in excellent agreement with earlier determinations.^{9,20} For ^{123}In and ^{125}In the differences between the Q_β values for the isomeric states and the ground states are 0.25 ± 0.22 and 0.18 ± 0.14 MeV, respectively, in agreement with the expected value of about 300 keV.¹³

The FK plots of β spectra corresponding to the gates 1335 and 188 keV for the isomers of ^{125}In are shown in Fig. 5.

2. Nuclides ^{127}In and ^{129}In

The decay properties of ^{127}In and ^{129}In , investigated by de Geer and Holm,¹⁴ are similar to those found for $^{121,123,125}\text{In}$. The main β transition from the ground state of ^{127}In feeds the level at 1602 keV in ^{127}Sn , while the isomeric state feeds a level

at 257 keV. For the ^{129}In case the analogous levels in ^{129}Sn are 2119 and 315 keV (see Fig. 4).

Method II was used for this experiment since the activity was too low to permit $\beta\gamma$ coincidences with Si(Li) and Ge(Li) detectors. The γ gates and the measured β end-point energies are given in Table I. The resulting Q_β values are $^{127}\text{In}^g$, $Q_\beta = 6.49 \pm 0.07$ MeV, $^{127}\text{In}^m$, $Q_\beta = 6.65 \pm 0.18$ MeV, $^{129}\text{In}^g$, $Q_\beta = 7.60 \pm 0.12$ MeV, and $^{129}\text{In}^m$, $Q_\beta = 7.8 \pm 0.6$ MeV.

Fermi-Kurie plots of the β spectra in coincidence with the gates at 1597 and 2119 keV in ^{127}Sn and ^{129}Sn are shown in Fig. 6.

B. Even-mass indium isotopes

Investigations of the decay properties of even-mass indium isotopes are in progress.^{15,21} Some pieces of information from these studies and from Refs. 22 and 23 needed for the discussion below are collected in Fig. 7.

Three isomers are found in each of the nuclides ^{120}In and ^{122}In , and two isomers in ^{124}In , ^{126}In , and ^{128}In .²¹ The 7^- states in $^{120-128}\text{Sn}$ are presumably isomeric with a delay of importance for the coincidence experiments.¹⁵

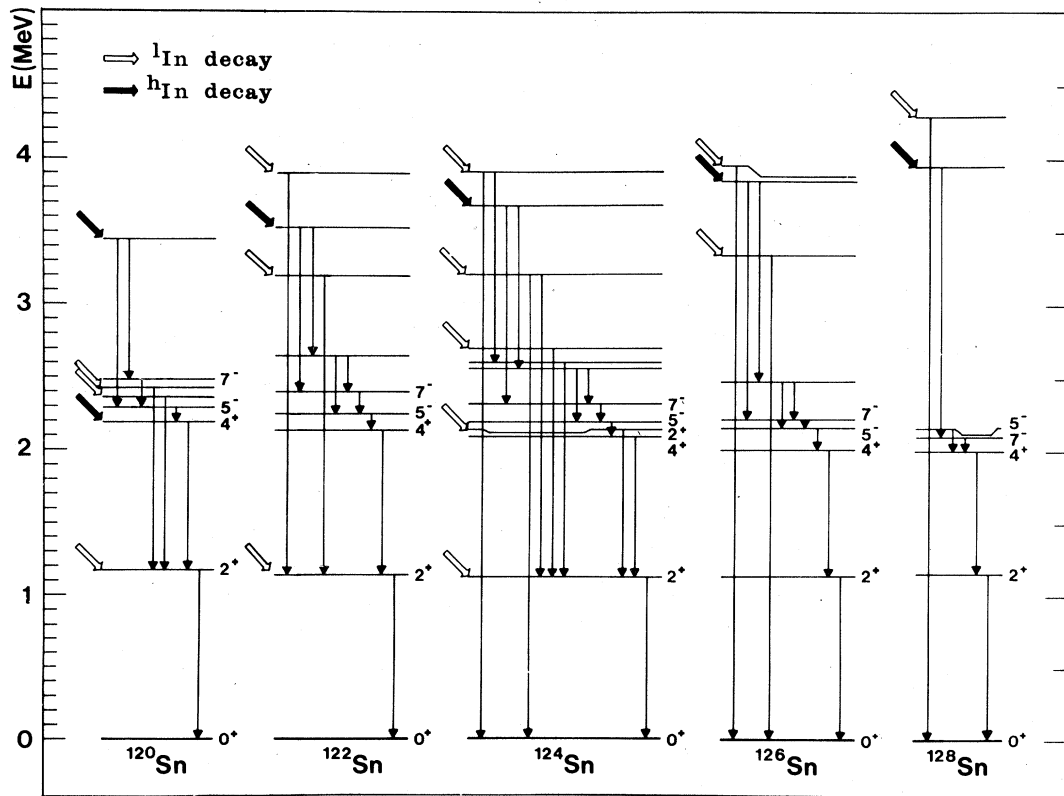


FIG. 7. Partial level schemes for even-mass tin isotopes. The superscripts l and h stand for "low spin" and "high spin," respectively.

TABLE II. Results of FK analyses for even-mass indium isotopes ^{120}In , ^{122}In , ^{124}In , ^{126}In , and ^{128}In .

Nuclide	Method	Half-life (s)	Gate energy (keV)	Level (keV)	Range of fit (MeV)	E^{max} (MeV)	Q_{β} value (MeV)	Mean Q_{β} value (MeV)	Other experimental determinations (MeV)
$^{120}\text{In}^{\text{a}}$	I	3.2 ^a	1171	1171 ^b	3.2-4.2	4.26 ± 0.29	5.43 ± 0.20	5.30 ± 0.17	5.6 ± 0.6 ^c
	III		1171	1171 ^b	1.4-3.5	4.06 ± 0.25	5.23 ± 0.25		
	III		1186	2358 ^b	1.0-2.4	2.76 ± 0.72	5.12 ± 0.72		
	III		1251	2423 ^b	0.6-2.6	2.97 ± 0.75	5.39 ± 0.25		
$^{120}\text{In}^{\text{b}}$	I	45 ^a	2195	2195 ^b	1.5-3.0	3.10 ± 0.20	5.30 ± 0.20	5.34 ± 0.17	5.3 ± 0.2 ^c
	III		965	3440 ^b	1.0-2.0	2.08 ± 0.40	5.52 ± 0.40		
$^{122}\text{In}^{\text{c}}$	III	1.5 ^d	2065	3206 ^b	0.7-2.7	3.57 ± 0.60	6.77 ± 0.60	6.51 ± 0.23	6.5 ± 0.2 ^e
	III		2759	3899 ^b	0.8-2.1	2.55 ± 0.40	6.45 ± 0.40		
	III		1141	1141 ^b	3.0-4.6	5.34 ± 0.36 ^f	6.48 ± 0.33		
	III								
$^{122}\text{In}^{\text{b}}$	III	10 ^a	878	3530 ^b	0.8-2.8	3.40 ± 0.40	6.93 ± 0.40	6.59 ± 0.18	6.6 ± 0.2 ^e
	III		1122	3530 ^b	1.2-2.8	2.98 ± 0.20	6.51 ± 0.20		
$^{124}\text{In}^{\text{g}}$	I, III	3.2 ^g						7.18 ± 0.05 ^h	
$^{124}\text{In}^{\text{h}}$	III	2.4 ^g						7.37 ± 0.21 ^h	
$^{126}\text{In}^{\text{i}}$	II	2.1 ⁱ	3345	3345 ⁱ	2.0-4.7	4.84 ± 0.19	8.19 ± 0.19	8.21 ± 0.08	
	III		3345	3345 ⁱ	2.0-4.7	4.98 ± 0.12	8.33 ± 0.12		
	III		3888	3888 ⁱ	2.1-4.2	4.23 ± 0.11	8.12 ± 0.11		
$^{126}\text{In}^{\text{b}}$	II	1.55 ⁱ	1637	3856 ⁱ	1.6-4.0	4.20 ± 0.17	8.06 ± 0.17		
$^{128}\text{In}^{\text{j}}$	II	0.9 ⁱ	4300	4300 ⁱ	1.2-4.8	4.98 ± 0.18	9.28 ± 0.18	9.31 ± 0.16	
	II		4300	4300 ⁱ	2.0-4.8	5.10 ± 0.34	9.40 ± 0.34		
$^{128}\text{In}^{\text{b}}$	II	0.9 ⁱ	1867	3963 ⁱ	1.9-5.4	5.43 ± 0.22	9.39 ± 0.22		

^aReference 21. ^bReference 22. ^cReference 25. ^dReference 18. ^eReference 23.
^fThe β spectrum corresponding to the gate at 1141 keV also contains a component of energy 3.0 MeV belonging to the decay of the 10 s isomer.
^gReference 24. ^hSee Table III. ⁱReference 15.

1. Nuclide ^{120}In

The half-lives of the β -decaying isomers of ^{120}In have been determined to be 3.2 s for the 1^+ state and 45 s for the $(4^+, 5^+)$ and the (8^-) states.²¹ The 3.2 s isomer decays mainly to the ground state of ^{120}Sn , the feeding to the 1170 keV level being about 13%.²² The lowest level fed by the $(4^+, 5^+)$ isomer is that at 2195 keV. The energy difference between the two 45 s isomers is smaller than the limits of error in the present investigation.

Using method I two γ gates were chosen at 1171 and 2195 keV (the latter is a sum peak). These gates correspond to levels in ^{120}Sn populated in the decay of the 1^+ isomer and the $(4^+, 5^+)$ isomer, respectively. The Q_β values thus obtained are 5.43 ± 0.20 MeV for $^{120}\text{In}^l$ and 5.30 ± 0.20 MeV for $^{120}\text{In}^h$, where "l" stands for "low spin" and "h" for "high spin".

With a Ge(Li) detector in the coincidence system (method III), gates were chosen at 1171, 1186, and 1251 keV corresponding to levels at 1171, 2423, and 2358 keV, respectively. All these transitions appear in the decay of the 3.2 s isomer. The resulting Q_β value was found to be 5.23 ± 0.22 MeV. In the decay of the high-spin isomers in ^{120}In only the γ gate at 965 keV, depopulating a level at 3440 keV, has been used for the determination of the total decay energy. The resulting Q_β value is 5.52 ± 0.40 MeV.

The average of the Q_β values obtained by the two different methods are $^{120}\text{In}^l$: $Q_\beta = 5.30 \pm 0.17$ MeV, and $^{120}\text{In}^h$: $Q_\beta = 5.34 \pm 0.17$ MeV. (See Table II.)

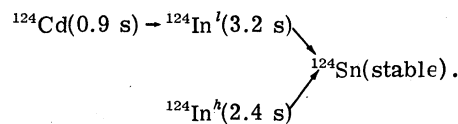
2. Nuclide ^{122}In

The half-lives of the three isomers in ^{122}In have been determined to be 1.5 s for the 1^+ isomer and 10 s for the $(4^+, 5^+)$ and (8^-) isomers.²¹

Using method III the Q_β value of the low-spin isomer was determined from the β end-point energies of the spectra corresponding to γ gates at 2065, 2759, and 1114 keV, depopulating levels at 3206, 3899, and 1141 keV, respectively (cf. Table II). In the decay of the high-spin isomers γ transitions of energies 878 and 1122 keV were chosen as gates. These transitions depopulate the level at 3530 keV. The resulting Q_β values are $^{122}\text{In}^l$: $Q_\beta = 6.51 \pm 0.23$ MeV, and $^{122}\text{In}^h$: $Q_\beta = 6.59 \pm 0.18$ MeV, in good agreement with earlier result 6.5 ± 0.2 and 6.6 ± 0.2 MeV for the low-spin and high-spin isomers of ^{122}In , respectively.²³ The difference between the two high-spin isomers is too small to be determined with this technique.

3. Nuclide ^{124}In

The nuclide ^{124}In belongs to the following isobaric chain^{15,24}:



The half-lives have been determined by means of γ counting.²⁴

The low-spin isomer is known to decay with feeding to the levels at 2130, 3215, and 3920 keV in ^{124}Sn . The levels at 2571 and 3688 keV are fed in the decay of $^{124}\text{In}^h$.

The γ transition from the 3215 keV state to the ground state gives rise to a rather strong peak in the γ spectrum in an energy region where the background is low. It is therefore well suited as a gate using method I. With the same method a γ gate was also chosen around 1132 keV, but the situation is here more complicated since double escape peaks from three lines around 2150 keV are also present.

A second experiment with method III was performed, and the results of the β end-point energies and the γ gates are collected in Table III together with results obtained with method I. The Q_β value of the high-spin isomer was obtained by measuring the β spectrum coincident with γ transitions from the 3688 keV level. The β spectra coincident with transitions from the level at 2571 keV had the same β end-point energies as those depopulating the 3688 keV level, indicating that the β particles mainly feed the latter level. The results are given in Table III.

The mean values of the Q_β determinations are $^{124}\text{In}^l$: $Q_\beta = 7.18 \pm 0.05$ MeV, and $^{124}\text{In}^h$: $Q_\beta = 7.37 \pm 0.21$ MeV.

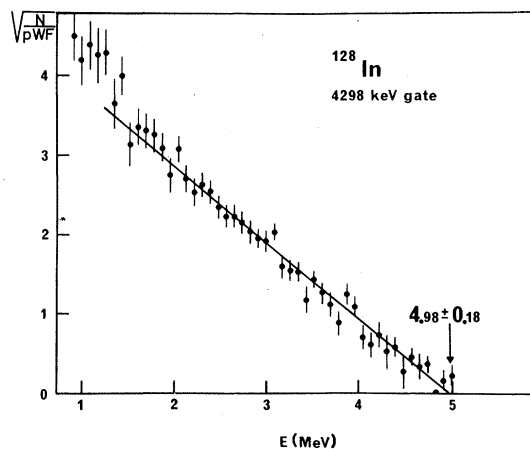


FIG. 8. Fermi-Kurie plot of the β spectrum corresponding to the gate at 4300 keV in the decay of $^{128}\text{In}^l$

TABLE III. Summary of Q_β determination for $^{124}\text{In}^l$ ($T_{1/2} = 3.2$ s) and $^{124}\text{In}^h$ ($T_{1/2} = 2.4$ s).

Isomer	Method	Gate energy (keV)	Level (keV)	Range of fit (MeV)	E_β^{max} (MeV)	Q_β value (MeV)
3.2 s	III	997	2130	2.4-5.0	5.10 ± 0.15	7.23 ± 0.15
	III	1315	3920	1.0-3.0	3.39 ± 0.26	7.31 ± 0.26
	III	1471	2604	1.4-3.1	3.46 ± 0.24	
	III	1572	2705	1.6-3.1	3.82 ± 0.66	
	III	2083	3215	0.6-3.6	4.01 ± 0.31	7.23 ± 0.31
	III	3215	3215	1.3-3.7	3.97 ± 0.16	7.19 ± 0.16
	I	3215	3215	1.6-3.6	3.92 ± 0.12	7.14 ± 0.12
	III	2703 ^a	3215	0.6-3.6	3.94 ± 0.25	7.16 ± 0.25
	I	2703 ^a	3215	2.5-3.6	3.94 ± 0.12	7.16 ± 0.12
	I	2192 ^b	3215	2.5-3.6	3.92 ± 0.09	7.14 ± 0.09
Mean value:						7.18 ± 0.05
2.4 s	III	244	2571	1.0-3.1	3.50 ± 0.32	
	III	364	2571	1.5-3.2	3.74 ± 0.24	
	III	1118	3688	1.2-3.2	3.66 ± 0.32	7.35 ± 0.32
	III	1361	3688	1.6-3.3	3.70 ± 0.29	7.39 ± 0.29
Mean value:						7.37 ± 0.21

^aSingle escape. ^bDouble escape.

4. Nuclides ^{126}In and ^{128}In

The half-lives of the different isomers of the nuclides ^{126}In and ^{128}In are given in Table II. The high-spin isomers were studied by setting γ gates around the 1637 keV transition depopulating the 3856 keV level in ^{126}In (directly or as a cascade) and around the 1867 keV transition depopulating the 3963 keV level in ^{128}In .²¹

In order to increase the coincidence rate for these very short-lived activities the experiments were performed with the method II. The results from the FK plots of the various β spectra are collected in Table II, and a FK plot of the β spectrum corresponding to the gate at 4300 keV in the decay of $^{128}\text{In}^l$ is shown in Fig. 8. The results for the different isomers are $^{126}\text{In}^l Q_\beta = 8.21 \pm 0.08$ MeV, $^{126}\text{In}^h Q_\beta = 8.06 \pm 0.17$ MeV, $^{128}\text{In}^l Q_\beta = 9.31 \pm 0.16$ MeV, and $^{128}\text{In}^h Q_\beta = 9.39 \pm 0.22$ MeV.

IV. DISCUSSION

A. Q_β values

In the following, the Q_β values for the ground states of the odd-mass indium isotopes will be discussed. The results for the even-mass isotopes are not accurate enough to establish the relative position of the isomers. The low-spin isomers of even-mass isotopes are fed in the decay of even-mass cadmium isotopes and, consequently, their mass excesses should be used when determining

the mass excesses for cadmium isotopes by the indirect Q_β method.

As predicted Q_β values are often used in calculations of $\log ft$ values, β strength functions, delayed neutrons, the r process of nucleosynthesis, etc., it is interesting to compare the experimental results with predicted values. In the comparison with predictions from mass formulas, three different types of formulas are chosen, namely, the droplet models of Myers,^{26(a)} Groote, Hilf, and Takahashi,^{26(b)} and Seeger and Howard,^{26(c)} the semiempirical shell model of Liran and Zeldes,^{26(d)} and the empirical mass relations of Comay and Kelson,^{26(e)} Jänecke *et al.*,^{26(f)} and Garvey *et al.*²⁷ The experimental values and the corresponding deviation in the predictions are compiled in Table IV. The mean experimental error for the complete series $^{120-129}\text{In}$ is 0.11 MeV, and the root-mean-square deviations for the mass formulas used in the comparison vary between 0.18 and 0.77 MeV (see Table IV). The droplet model predictions are less accurate than the others for these nuclides. It should be remembered, however, that they use fewer coefficients than the other formulas.

B. Masses

The mass excesses of $^{120-126}\text{Sn}$ and $^{127-129}\text{Sn}$ are known from Refs. 9 and 28, respectively. By adding the Q_β values from Table IV to these mass ex-

TABLE IV. Summary of Q_β values obtained in the present work and comparison with different mass formulas productions.

Nuclide	Q_β value (MeV)	$Q_{\beta,\text{exp}} - Q_{\beta,\text{pred}}$ (MeV)						
		a	b	c	d	e	f	g
$^{120}\text{In}^f$	5.30 ± 0.17	0.61	0.95	0.47	-0.04	0.06	-0.07	-0.11
$^{121}\text{In}^g$	3.41 ± 0.05	0.24	0.36	0.58	-0.21	0.15	0.02	-0.13
$^{122}\text{In}^f$	6.51 ± 0.23	0.84	1.13	0.60	0.36	0.31	0.16	-0.04
$^{123}\text{In}^g$	4.44 ± 0.06	0.33	0.38	0.41	-0.16	0.20	0.07	0.06
$^{124}\text{In}^f$	7.18 ± 0.05	0.61	0.83	0.29	-0.04	0.12	-0.01	-0.17
$^{125}\text{In}^g$	5.48 ± 0.08	0.44	0.43	0.35	-0.01	0.24	0.20	0.01
$^{126}\text{In}^f$	8.21 ± 0.08	0.75	0.90	0.24	0.30	0.25	0.25	0.05
$^{127}\text{In}^g$	6.49 ± 0.07	0.56	0.48	0.24	0.20	0.27	0.32	0.12
$^{128}\text{In}^f$	9.31 ± 0.16	0.98	1.06	0.44	0.60	0.58	0.59	0.39
$^{129}\text{In}^g$	7.60 ± 0.12	0.80	0.65	0.40	0.62	0.64	0.60	0.29
Root-mean-square deviation		0.65	0.77	0.42	0.33	0.33	0.31	0.18

^aReference 26(a).^bReference 26(b).^cReference 26(c).^dReference 26(d).^eReference 26(e).^fReference 26(f).^gReference 27.

cesses, the mass of $^{120-129}\text{In}$ were deduced. The resulting masses are compared to mass predictions^{26(a)-26(f),27} in Table V.

The mean experimental error for the indium isotopes studied are 0.11 MeV, and the predictions deviate, on average, by 0.21 to 1.36 MeV.

The formulas of Liran and Zeldes, Comay and Kelson, and Garvey *et al.* give, in general, predictions with acceptable precision. Among the droplet model formulas, the Seeger-Howard one reproduces the experimental masses well. Before drawing any conclusions about which droplet

TABLE V. Summary of experimental mass excesses obtained for $^{120-129}\text{In}$ and comparisons with different mass formulas predictions.

Nuclide	Mass excess (MeV)	$M_{\text{exp}} - M_{\text{pred}}$ (MeV)						
		a	b	c	d	e	f	g
^{120}In	-85.80 ± 0.17	1.36	1.35	-0.50	-0.01	0.18	-0.08	-0.10
^{121}In	-85.79 ± 0.05	1.36	1.30	0.60	0.04	0.28	-0.01	-0.17
^{122}In	-83.44 ± 0.23	1.20	1.10	1.04	0.22	0.03	0.15	-0.55
^{123}In	-83.38 ± 0.06	1.44	1.26	0.22	0.04	0.41	0.09	-0.02
^{124}In	-81.06 ± 0.05	1.45	1.20	0.04	-0.02	0.25	-0.04	-0.15
^{125}In	-80.42 ± 0.08	1.46	1.08	0.08	0.12	0.38	0.21	0.05
^{126}In	-77.81 ± 0.09	1.18	0.69	-0.61	-0.15	-0.04	0.31	-0.21
^{127}In	-77.02 ± 0.07	1.34	0.69	-0.32	0.19	0.11	0.37	0.14
^{128}In	-74.00 ± 0.17	1.49	0.70	-0.30	0.42	0.24	0.66	0.33
^{129}In	-73.03 ± 0.17	1.25	0.26	-0.53	0.37	0.05	0.64	0.16
Root-mean-square deviation		1.36	1.02	0.39	0.21	0.24	0.34	0.24

^aReference 26(a).^bReference 26(b).^cReference 26(c).^dReference 26(d).^eReference 26(e).^fReference 26(f).^gReference 27.

TABLE VI. Values of the "neutron window" deduced from experimental mass data.

Precursor	Q_β (MeV)	Emitter	Mass excess (MeV)	B_n (MeV)	Neutron window $Q_\beta - B_n$ (MeV)
		^{123}Sn	-87.82 ± 0.004^a		
^{124}In	7.18 ± 0.05	^{124}Sn	-88.24 ± 0.01^a	8.49 ± 0.01	-1.31 ± 0.05
^{125}In	5.48 ± 0.08	^{125}Sn	-85.90 ± 0.01^a	5.73 ± 0.01	-0.25 ± 0.08
^{126}In	8.21 ± 0.08	^{126}Sn	-86.02 ± 0.01^a	8.19 ± 0.01	0.02 ± 0.08
^{127}In	6.49 ± 0.07	^{127}Sn	-83.50 ± 0.03^b	5.55 ± 0.03	0.94 ± 0.07
^{128}In	9.31 ± 0.16	^{128}Sn	-83.31 ± 0.06^b	7.87 ± 0.06	1.44 ± 0.13
^{129}In	7.60 ± 0.12	^{129}Sn	-80.63 ± 0.12^b	5.39 ± 0.13	2.21 ± 0.17

^aReference 9. ^bReference 28.

formula is to be used far away from stability, we recapitulate the results²⁸ from mass determinations of neutron-rich tin, antimony, and tellurium isotopes. For these isotopes Myers gives the best predictions (mean deviation 0.32 MeV) while Seeger and Howard and Groote *et al.*, on the average, predict the masses to be 1.0 and 0.87 MeV, less bound than found experimentally. Apparently, the estimates using the formula of Groote *et al.* are less precise both for isotopes with $Z < 50$ and $Z \geq 50$. Myers' predictions are very good for the region $Z \geq 50$, but the failure in the predictions for $^{120-129}\text{In}$ is grave. This leads us to conclude that, as for neutron-rich zinc, gallium, germanium, and arsenic isotopes,²⁹ the best droplet mass formula for extrapolations far away from stability in the region studied seems to be the one of Seeger and Howard.

C. Predictions about delayed-neutron precursors

In general, predictions concerning the occurrence of delayed-neutron emission are based on mass formula estimates because experimental neutron binding energies are scarce in regions far from stability, and experimental Q_β values

are often lacking. The present investigation makes the situation favorable for predictions about delayed-neutron precursors among the indium isotopes based on experimental mass data.

These data have been used to calculate the neutron window $|Q_\beta - B_n|$ for $^{124-129}\text{In}$. The results are collected in Table VI. From this table it is seen that ^{124}In and ^{125}In cannot be delayed-neutron precursors, and that ^{126}In is a doubtful case. In an investigation at this laboratory no delayed neutrons were found at these mass numbers.¹⁹ On the other hand, ^{127}In , ^{128}In and ^{129}In were shown to be neutron precursors in agreement with the positive neutron windows found for those cases.

ACKNOWLEDGMENTS

The authors are grateful to Dr. B. Fogelberg for submitting to us results prior to publication and for interesting discussions. For excellent isotope separator performance L. Jacobsson, B. Johansson, and O. Johansson are gratefully acknowledged. This work was supported by the Swedish Council for Atomic Research.

¹W. L. Talbert, in Proceedings of the International Conference on the Properties of Nuclei far from the Region of Beta-Stability, Leysin, 1970 (unpublished) p. 109, [CERN Report No. CERN-70-30, 1970 (unpublished)].

²C. Thibault, in Proceedings of the Third International Conference on Nuclei far from Stability, Cargèse, 1976 (unpublished), p. 93, [CERN Report No. CERN 76-13, 1976 (unpublished)].

³D. N. Schramm and E. B. Norman, in Proceedings of the Third International Conference on Nuclei far from Stability, Cargèse, 1976 (see Ref. 2), p. 570.

⁴S. Borg, I. Bergström, G. B. Holm, B. Rydberg, L.-E. De Geer, G. Rudstam, B. Grapengiesser,

E. Lund, and L. Westgaard, Nucl. Instrum. Methods **91**, 1 (1971).

⁵Ch. Andersson, B. Grapengiesser, and G. Rudstam, in Proceedings of the Eighth International EMIS Conference, Skövde, 1973 (unpublished), p. 463.

⁶G. Andersson, B. Hedin, and G. Rudstam, Nucl. Instrum. Methods **28**, 245 (1964).

⁷E. Lund and G. Rudstam, Nucl. Instrum. Methods **133**, 173 (1976).

⁸K. Aleklett, Ph.D. thesis, University of Gothenburg, Sweden, 1977 (unpublished).

⁹A. H. Wapstra and K. Bos, Nucl. Data Tables **19**, 175 (1977).

¹⁰M. J. Berger, S. M. Seltzer, S. E. Chappell, J. C.

- Humphreys, and J. W. Motz, Nucl. Instrum. Methods 69, 181 (1969).
- ¹¹G. Hedin and A. Bäcklin, Ark. Fys. 38, 593 (1969).
- ¹²B. Fogelberg, L.-E. De Geer, K. Fransson, and M. af Ugglas, Z. Phys. A276, 381 (1976).
- ¹³C. V. Weiffenbach and R. Tickle, Phys. Rev. C 3, 1668 (1971).
- ¹⁴L.-E. De Geer and G. B. Holm, Research Institute for Physics Annual Report, 1974 (unpublished), p. 102.
- ¹⁵B. Fogelberg and P. Carlé, in Proceedings of the International Conference on Nuclear Structure, Tokyo, 1977 (unpublished), p. 363.
- ¹⁶A. Kerek, G. B. Holm, S. Borg, and P. Carlé, Nucl. Phys. A209, 520 (1973).
- ¹⁷A. Kerek, G. B. Holm, L.-E. De Geer, and S. Borg, Phys. Lett. 44B, 252 (1973).
- ¹⁸B. Grapengiesser, E. Lund, and G. Rudstam, J. Inorg. Nucl. Chem. 36, 2409 (1974).
- ¹⁹E. Lund and G. Rudstam, Phys. Rev. C 13, 1544 (1976).
- ²⁰R. L. Auble, Nucl. Data Sheets 7, 363 (1972).
- ²¹B. Fogelberg, private communication.
- ²²E. Liukkonen and J. Hattula, Z. Phys. 241, 150 (1971).
- ²³K. Takahashi, D. L. Swindle, and P. K. Kuroda, Phys. Rev. C 4, 517 (1971).
- ²⁴B. Fogelberg, T. Nagarajan, and B. Grapengiesser, Nucl. Phys. A230, 214 (1974).
- ²⁵J. Kantele and M. Karras, Phys. Rev. 135, B9 (1964).
- ²⁶(a) W. D. Myers, At. Data Nucl. Data Tables 17, 411 (1976); LBL Report No. LBL-3428, 1974 (unpublished); (b) H. V. Groote, E. R. Hilf and K. Takahashi, *ibid.* 17, 418 (1976); (c) P. A. Seeger and W. M. Howard, *ibid.* 17, 428 (1976); LA Report No. LA-5750, 1974 (unpublished); (d) S. Liran and N. Zeldes, *ibid.* 17, 431 (1976); (e) E. Comay and I. Kelson, *ibid.* 17, 463 (1976); (f) J. Jänecke, *ibid.* 17, 455 (1976).
- ²⁷G. T. Garvey, W. J. Gerace, R. L. Jaffe, I. Talmi, and I. Kelson, Rev. Mod. Phys. 41, S1 (1969).
- ²⁸E. Lund, K. Aleklett, and G. Rudstam, Nucl. Phys. A286, 403 (1977).
- ²⁹K. Aleklett, E. Lund, and G. Rudstam, Nucl. Phys. A285, 1 (1977).